

# SHINING LIGHT ON PRECISION: UNRAVELING XBPMs AT THE AUSTRALIAN SYNCHROTRON

B. Lin<sup>†</sup>, J. McKinlay, S. Porsa, Y. E. Tan, ANSTO, Australian Synchrotron, Melbourne, Australia

## Abstract

At the Australian Synchrotron (AS), the need for non-destructive X-ray beam positioning monitors (XBPM) in the beamline front ends led to the development and installation of an in-house prototype using the photoelectric effect in 2021. This prototype served as a proof of concept and an initial step towards creating a customised solution for real time X-ray position monitoring. Of the new beamlines being installed at the AS, the High-Performance Macromolecular Crystallography (MX3) and Nanoprobe beamlines require XBPMs due to their small spot size and high stability requirements. However, a significant hurdle is the short distance from the source point to the XBPM location, resulting in an extremely restricted aperture to accurately monitor the beam position. Scaling down the photoelectric prototype to accommodate the available space has proven challenging, prompting us to explore alternative designs that utilize temperature-based methods to determine the beam position. This paper details insights made from investigating this alternative method and design.

## INTRODUCTION

X-ray beam positioning monitoring technology plays an important role in synchrotron facilities, gaining increasing significance as light sources move towards smaller source sizes and nanoscale sample probing. The AS has been exploring this technology to develop an in-house, non-destructive white beam XBPM catered to its light source requirements. A photoemission XBPM was designed and installed by 2021 on the optical diagnostic beamline (ODB) as a proof of concept and prototype for future beamlines. The design was derived from LNL and Soleil XBPM designs [1, 2]. However, there have been challenges with scaling this prototype to the new beamlines that need an XBPM due to their small spot size and high stability requirements, namely the Nanoprobe and MX3 beamline. Consequently, there has been a need to investigate alternative methods and designs that can cater for the requirements and specifications for the two beamlines.

## PHOTOEMISSION XBPM

A photoemission prototype XBPM was fabricated and installed on the ODB with these requirements in consideration:

- Drain current from a single XBPM blade needs to be a minimum of 2  $\mu\text{A}$  at 200 mA [3].
- Position resolution of  $< 1 \mu\text{m}$  for an undulator source at nominal beam current of 200 mA.
- Misalignment tolerance in the insertion device (ID) source point of  $\pm 0.5 \text{ mrad}$  in both planes.

<sup>†</sup> becky.lin@ansto.gov.au

## XBPM Prototype Using Photoemission

The final design and assembly before the last flange was fastened can be seen below in Fig. 1 with the respective beam direction in red.

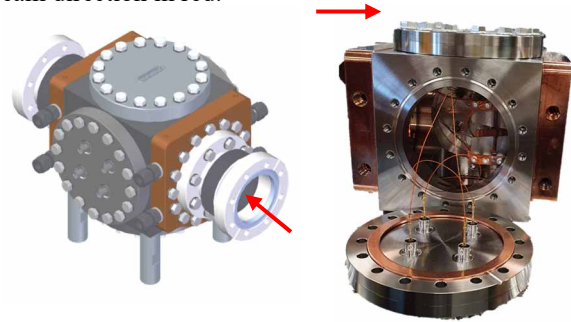


Figure 1: Final render and assembly of XBPM prototype.

The body is an ultra-high vacuum (UHV) stainless steel cube with flanged faces. Looking from upstream, the blades are mounted to the rear flange, the front flange has a pinhole mask for the beam fringes, the left and right flange both have four triaxial feedthroughs to pick up the drain current from the blades, and the top flange has a D-sub miniature (D-sub) port for temperature monitoring of the XBPM. The front and rear face of XBPM is shown in Fig. 2.

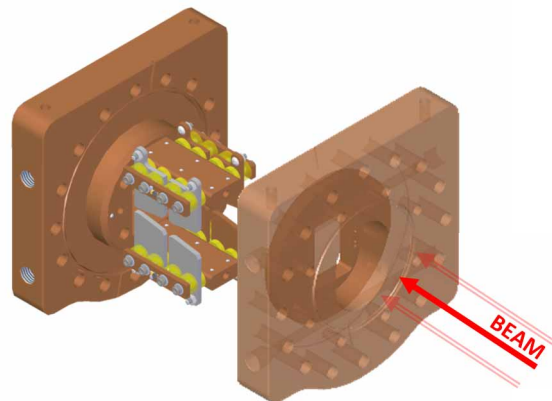


Figure 2: Front and rear flange of XBPM.

The pinholes in the mask have a diameter of 2 mm that allow the beam fringes to pass through. Theoretically, it samples the beam distribution more accurately as it strikes a more specific part of the blade, as this enables sampling of the beam at fixed points in space with a well-defined size. This allows a beam distribution to be fitted through the collected data more accurately and determine a verified centre point of the beam. Figure 3 exhibits the front view of the mask, where the pinholes are the four smaller holes adjacent to the centre window.

Content from this work may be used under the terms of the CC-BY-4.0 licence (© 2023). Any distribution of this work must maintain attribution to the author(s), title of the work, publisher, and DOI

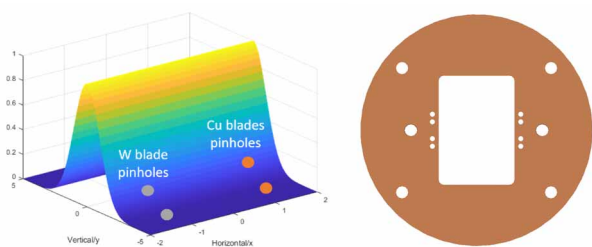


Figure 3: Beam distribution with pinhole samples and front view of XBPM mask.

Two blade materials were used, copper (Cu) and tungsten (W), to test any differences in sensitivity or accuracy. Figure 4 reveals the resolution of the prototype compared to the storage ring radio frequency (RF) BPM with fast orbit feedback disabled on the left side and after feedback is enabled on the right.

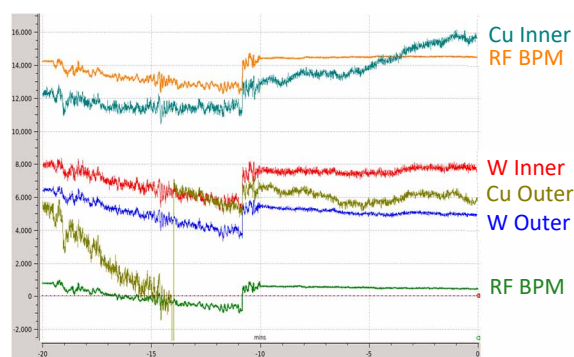


Figure 4: BPM signal level vs time.

The position resolution achieved is  $< 200$  nm and short-term drifts appear to be  $< 2$   $\mu$ m over 10 minutes, whilst long term drifts were much larger, over a few hours, and were significantly dependent on beam current and temperature stability of low conductivity water (LCW) supply.

### Limitations of XBPM Prototype

Even though, the results of the prototype seemed promising, given the aperture imposed by the first mask in the new beamlines, it has resulted in an extremely restricted orifice to accurately monitor beam position. Therefore, scaling down the photoemission prototype proved unrealistic due to space constraints. The beam fringes will be approximately 2.3 keV in the given area for the blade positions, which is around 8 x 6 mm and permitting the critical beam area of 2 x 1.5 mm in the centre. This prompted an investigation for different technologies to downscale.

Both photoemission and auger electron emission are surface layer processes therefore a thin film coating is sufficient and equivalent in signal intensity to a solid metal blade.

## EXPERIMENTATION

Various trials were performed to determine if there was a viable method of creating “blades” from thin film coating. Laser cutting a diamond wafer was conducted to observe its feasibility to create unique shapes for assembly and design purposes.

### Thin Film Coating

The first tests seen in Fig. 5 were two Cu blocks polished to 30 nm, coated in 500 nm of alumina ( $Al_2O_3$ ) as an insulation layer, then a layer of 100 nm of gold (Au). The technique applied was electron beam (e-beam) deposition and differing Au widths were trialled to simulate varying “blade” thicknesses.

Secondly, in Fig. 5, a silicon wafer was similarly coated with 500 nm of Cu, then 500 nm of  $Al_2O_3$  and 100 nm of Au, as prepared in the previous test. This was performed to assess the level of surface polishing required, as the silicon wafer emulates a near optimal polished Cu surface.

X-ray photoelectron spectroscopy (XPS) was used to analyse the sufficiency of thin film thickness and measure the drain current from Au.

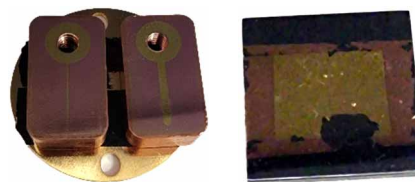


Figure 5: First and second test pieces.

The final coat test applied a strip of 100 nm thick Au on a diamond wafer to determine if there was an adequate drain current detected from the thin film.

### Laser Cutting Diamond

A 2 mm hole was laser cut with a YAG laser type through an optical grade chemical vapour deposition (CVD) diamond wafer and the cut precision was observed.

## RESULTS AND DISCUSSION

In Fig. 6, the first test result, with a photon energy level at 1.99 keV, produced a resolution of 200  $\mu$ m with the drain current from Au, peaking at around 2 nA both at 400 sec and 700 sec for the two “blade” thicknesses. The insulating layer had an average of 0.7 nA and thus giving a differentiating factor of 2.86.

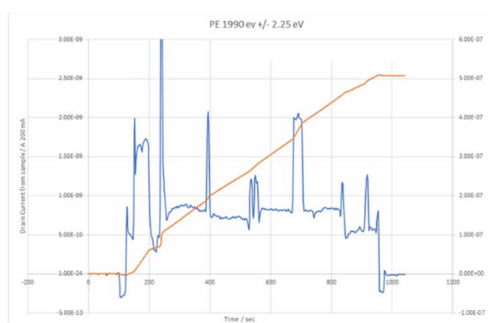


Figure 6: Drain and integrated current vs time.

The second test results proved better, with a photon energy level at 1.5 keV, as there was a drain current to insulator current ratio of 82.35, with Au peaking at 14 nA compared to the insulating layer of 0.17 nA.

This difference in the Au drain current to the insulating drain current ratio could be attributed to the polishing surface of the copper contrasted to the silicon surface.

Additionally, the XPS indicated Cu was visible on the Al<sub>2</sub>O<sub>3</sub> layer, which may suggest cavities in this layer.

Thirdly, the results in Fig. 7 revealed that the Au drain current average was 0.6 nA, opposed to the diamond drain current of 0.2 nA. The signal to noise ratio was suboptimal, and thus photoemission was discontinued as a viable option.

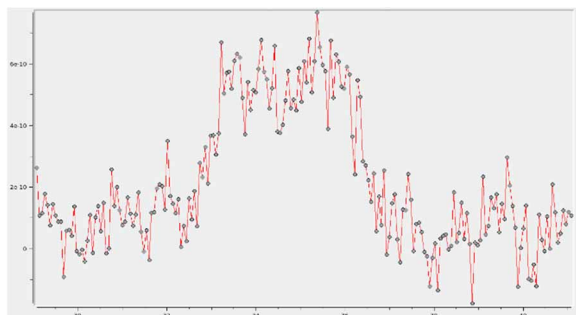


Figure 7: Drain current vs time.

Lastly, below in Fig. 8, it displays the uneven cut edge of the diamond and noticeable kerf after being laser cut.

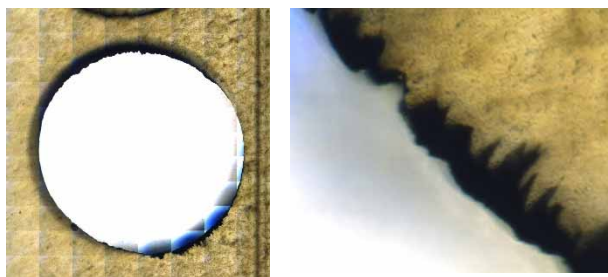


Figure 8: Laser cut diamond edges.

This result may increase stresses in the diamond when heated. It is intended that different laser cutting methods will continue to be investigated, such as newer laser cutting technology that utilises a waterjet stream simultaneously with the YAG laser which produces a cleaner edge [4].

### TEMPERATURE-BASED APPROACH

The AS is in the early stages of developing an XBPM using a temperature-based approach. It is inspired by RTD technology where an increase in temperature will cause an increase in electrical resistance. A current is passed through the sensor and resistance is measured through the voltage drop across the track. Figure 9 shows a PT100 scanned by AS Micro-Computed Tomography (MCT) beamline and a render of a preliminary track design on a diamond wafer.

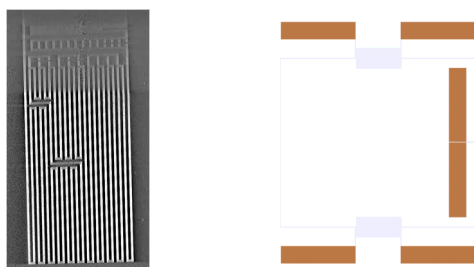


Figure 9: PT100 track and preliminary piece.

It is common for platinum (Pt) to be used as a track due to its wide temperature range, high melting point and stability over time. Diamond was selected as a substrate material as it had properties of high insulation and thermal conductivity. When the beam passes through the centre of the diamond, it will heat the middle while the sides of the wafer piece is being cooled by surrounding CuCrZr that is connected to LCW supply. The temperature sensor track will be coated on through photolithography. Early designs of this track for the XBPM is shown in Fig. 10.

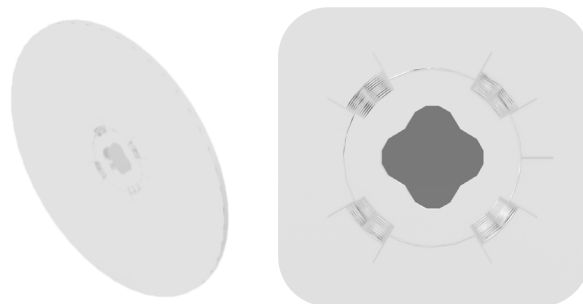


Figure 10: Early design of temperature-based approach.

The position of the beam will be determined by temperature, as there is a relatively linear relationship between thin film Pt resistivity and temperature [5].

Figure 11 shows both a finite element analysis (FEA) model of the diamond wafer and its temperature gradient in °C when the beam is going directly through the centre and when it is shifted 0.1 μm to the left.

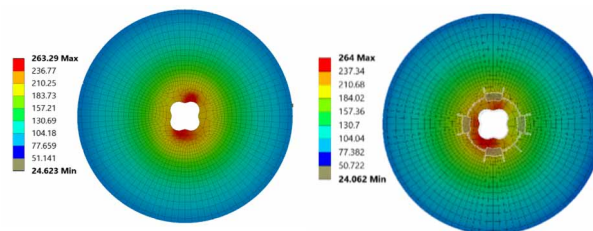


Figure 11: Beam travelling through the centre of piece (left) and beam with a 0.1 μm shift to the left (right).

This illustrates that there is a significant temperature change for a small movement in the beam as it is greater than 0.1 C change at the region of track placement. Some variables to also consider in the temperature-based approach are track material, size, and position for the best sensitivity.

### CONCLUSION

After developing a prototype XBPM using the photoelectric effect, it has been shown that there are constraints of scaling the model and effect. Through experiments with thin film, valuable insight of its application has been gained, in addition to the limitations of certain laser cutting methods for diamond. Currently, the aim is to explore and establish an XBPM that utilises thermal properties to its advantage and further investigate the realm of XBPM possibilities.

## ACKNOWLEDGEMENTS

This work was performed in part at the Melbourne Centre for Nanofabrication (MCN) in Victorian Node of the Australian National Fabrication Facility, University of Melbourne School of Physics Advanced Materials Laboratory, and AS beamline scientists from MCT (Benedicta Arhatari, Andrew Stevenson), Soft X-ray (Bruce Cowie, Anton Tadich) and Infrared (IR) (Annaleise Klein).

Thank you to those who have helped in the XBPM projects - Brian Jensen, Trent Smith, Jason Wirthensohn, Andy Starritt, Adrian Hawley, Emily Griffin, Chris Ampt and Brad Mountford.

## REFERENCES

[1] N. Hubert *et al.*, “Design of a new blade type X-BPM”, in *Proc. IBIC'14*, Monterey, CA, USA, Sep. 2014, paper WEPD22, pp. 687-690.

- [2] L.M. Volpe, “Blade XBPM optimizations for Sirius”, presented at *MEDSI'16*, Barcelona, Spain, Sep 2016, paper not published.
- [3] A. Kosicek and P. Leban, “Libera Brilliance and Libera Photon Working Together in Fast Orbit Feedback”, in *Proc. ICALEPCS'09*, Kobe, Japan, Oct. 2009, paper THP070, pp. 797-799.
- [4] Synova, <https://www.synova.ch/technology/synova-laser-microjet.html>
- [5] J. Kim, J. Kim, Y. Shin, and Y. Yoon, “A study on the fabrication of an RTD (resistance temperature detector) by using PT thin film”, *Korean J. Chem. Eng.*, vol. 18, no. 1, pp. 61-66, 2001. doi:10.1007/bf02707199